Two-Dimensional NMR of Diffusion Systems

Yi-Qiao Song, Lukasz Zielinski, and Seungoh Ryu

Schlumberger-Doll Research, 1 Hampshire Street, Cambridge, Massachusetts 02139, USA

(Received 26 March 2008; published 18 June 2008)

We consider diffusion in porous media with well-connected pore space for which isolated-pore models are insufficient. Explicit pore-to-pore exchange parameters were introduced in recent 2D NMR experiments. However, such parameters capture only certain aspects of the interpore spin dynamic which, for single-fluid saturated media, are wholly determined by diffusion. Here, we develop a theoretical approach suitable for a quantitative description of such 2D NMR taking a full account of the underlying diffusion modes. We use simple models of one pore and two coupled pores to demonstrate the rich behavior of 2D NMR.

DOI: 10.1103/PhysRevLett.100.248002 PACS numbers: 81.05.Rm, 66.10.cg, 82.56.−b

Connectivity of the pore space in sedimentary rocks plays a critical role in the flow of crude oils for petroleum extraction. Interconnection between different classes of pores in cements and concretes is critical for controlling its mechanical and chemical properties. A recent development of 2D NMR [1,2] has shown an exciting possibility of characterizing the diffusion of fluid from one pore to another in such systems. This is a significant progress beyond the conventional relaxation measurement (e.g., T_2), often employed to probe the pore geometry, as the latter does not probe the connectivity explicitly. The new experiments use T_1-T_2 and T_2-T_2 correlation spectroscopy [3,4] and found that the resulting 2D spectra show significant off-diagonal signals, which are interpreted as evidence of diffusion between different pores. The theoretical understanding of such experiments remains incomplete as the diffusion within pores is not treated on equal footing with the interpore diffusion that is described via a phenomenological hopping parameter. As the interpore coupling strengthens, the division of the pore space into intra- and interpore begins to lose grounds as does any interpretational scheme based on such division. Here we provide a general theoretical framework for understanding such 2D NMR for a porous media, which takes full account of the diffusion-based spin dynamics. We demonstrate that such a framework provides means to clarify and understand aspects of these experiments in a way free from the limited notion of an isolated pore and its variants.

The differential equation governing the evolution of the longitudinal (T_1) or the transverse (T_2) component of nuclear spin magnetization carried by diffusing molecules is the well-known Torrey-Bloch equation [5]:

$$\frac{\partial}{\partial t} m(\mathbf{r}, t) = D\nabla^2 m(\mathbf{r}, t) - \mu m(\mathbf{r}, t), \tag{1}$$

where D is the bulk diffusion constant and μ is the bulk spin relaxation rate. m is the magnetization deviation from its equilibrium. The detected signal is $M(t) = \int m(r, t) d\upsilon$. Suppressing the bulk relaxation, as it merely adds a constant decay rate, a solution can be found in the general form:

$$m(\mathbf{r}, t) = \sum_{n=0}^{\infty} a_n \phi_n(\mathbf{r}) e^{-t/T_n}, \tag{2}$$

where ϕ_n and T_n are eigenfunctions and eigenvalues of the Helmholtz equation

$$\phi_n(\mathbf{r})/T_n + D\nabla^2 \phi_n(\mathbf{r}) = 0, \tag{3}$$

with the mixed boundary condition at the pore surface: $D\hat{n} \cdot \nabla \phi_n + \rho \phi_n = 0$ for $\mathbf{r} \in \Sigma_p$ where $\hat{n}$ is the unit vector normal to the pore-matrix interface Σ_p and ρ is the surface relaxivity. The eigenfunctions are normalized by $(1/V_p) \int d\upsilon \phi_n^2 = 1$ where V_p is the pore volume. In the following, all volume integration should be understood to be over V_p, which is taken to be $V_p = 1$. The T_n and ϕ_n can represent the diffusion eigenvalues and eigenfunctions of either T_1 or T_2 processes depending on the experiment and will be denoted by $T_{1,n}$ and $\phi_{1,n}$ or $T_{2,n}$ and $\phi_{2,n}$, respectively. The two eigensystems are generally different as the surface relaxivity ρ assumes different values for the longitudinal (ρ_1) and the transverse (ρ_2) dynamics [6].

Using the completeness and orthogonality of the eigenmodes, the amplitude of each mode in the initial magnetization distribution $m(\mathbf{r}, 0)$ is given by

$$a_n = \int \phi_n^*(\mathbf{r}) m(\mathbf{r}, 0) d\upsilon. \tag{4}$$

Brownstein and Tarr [7] investigated the diffusion eigenmodes for *isolated* (*closed*) pores of elemental geometries such as sphere and rectangles, and an extensive body of literature exists that has applied their basic techniques to various systems. Ryu has further developed a quantum mechanics analogy that relates diffusion dynamics in an extended pore system to the spectroscopy in a disordered environment [8]. In general, the Helmholtz equation Eq. (3) is of fundamental importance in quantum mechanics, electromagnetics, and acoustics. The inverse problem of determining the geometry of the enclosing space from the measured eigenspectrum is at the heart of numerous

applications, and has stimulated much theoretical [9] and experimental [10,11] research.

We use the diffusion eigensystem to build a theoretical framework for experiments such as the $T_1 - T_2$ correlation shown schematically as

$$\underbrace{\pi - \tau_1}_{T_1 \text{ relaxation}} \underbrace{-\frac{\pi}{2} - t_e/2 - [\pi - t_e]_N}_{T_2 \text{ relaxation}}. \tag{5}$$

The first 180° pulse inverts the nuclear magnetization from its initial distribution initiating the T_1 relaxation. During this period, the magnetization dynamics are described by T_1 modes; thus, the magnetization at the end of the τ_1 period is

$$m(\mathbf{r}, \tau_1) = \sum_{p=0}^{\infty} a_p \phi_{1,p}(\mathbf{r}) e^{-\tau_1/T_{1,p}}, \tag{6}$$

and the coefficient is determined by magnetization right after the π pulse, $m(\mathbf{r}, 0)$. Since the rf tipping angle is uniform on the pore scale, we assume $m(\mathbf{r}, 0) = -1$.

After a period of time τ_1, a CPMG pulse sequence [12,13] is applied to rotate the magnetization from the axis along the external field to the transverse plane and record the transverse relaxation process. Neglecting the relaxation during rf pulses, the magnetization for the echo at τ_2 time (after the $\pi/2$ pulse)

$$m(\mathbf{r}, \tau_1, \tau_2) = \sum_{q=0}^{\infty} b_q \phi_{2,q}(\mathbf{r}) e^{-\tau_2/T_{2,q}}, \tag{7}$$

where $b_q = \int \phi^*_{2,q}(\mathbf{r}) m(\mathbf{r}, \tau_1) d\upsilon$. The detected signal is an integral of $m(\mathbf{r}, \tau_1, \tau_2)$ with the rf coil sensitivity, which is assumed to be unity. Then the T_1-T_2 correlation spectrum is obtained through two-dimensional Laplace inversion [14] of experimental data $m(\mathbf{r}, \tau_1, \tau_2)$ with respect to τ_1 and τ_2 and its amplitude in the T_1-T_2 domain will correspond to

$$S_{12}(T_1, T_2) = \sum_{p,q} \langle f|\phi_{2,q}\rangle\langle\phi_{2,q}|\phi_{1,p}\rangle\langle\phi_{1,p}|i\rangle \times \delta(T_1 - T_{1,p})\delta(T_2 - T_{2,q}), \tag{8}$$

using the standard bra-ket $\langle\,|\,\rangle$ of quantum mechanics for a compact and explicit accounting of the sequential order of operations. Note that $\langle\phi|\psi\rangle = \int d\upsilon \phi^*(\mathbf{r})\psi(\mathbf{r})$ and $|i\rangle$ and $|f\rangle$ represent the initial and the final distributions, which are both assumed to be uniform here. Experimentally, one may employ arbitrary distributions to obtain the S_{12} spectrum weighted differently.

There are two major features of the spectrum S_{12}. One originates from the modes with $p = q$ called diagonal features and others with $p \neq q$ called off-diagonal features. Since the longitudinal and transverse eigensystems are only different by surface relaxivity, the T_2 and T_1 modes are generally similar, particularly for higher modes. Thus the diagonal peaks are almost always stronger than the off-diagonal ones, which represent the extent of the *nonorthogonality* of T_2 and T_1 modes. Note also that if $\rho_2 = \rho_1$, no off-diagonal features should be expected in $T_1 - T_2$ experiments. Similarly, if both T_2 and T_1 are in a fast diffusion limit, e.g., $d\rho_{1,2}/D \ll 1$ (d is pore size), T_2 and T_1 modes are essentially the same and no off-diagonal features will be excited. We emphasize that this is the case regardless of the geometry of the pore space. A consequence made clear by this analysis is that, even if the pores are interconnected, for systems with $\rho_1 = \rho_2$, the $T_1 - T_2$ correlation spectrum will show no off-diagonal peaks. And conversely, in a single pore with different ρ_1 and ρ_2, off-diagonal peaks may be observed.

We now examine these notions with an example of one-dimensional pore of length L. Figure 1 shows its $T_1 - T_2$ spectrum, with $L\rho_1/D = 0.5$, $L\rho_2/D = 5$, and $L^2/D = 1$ s. We define $K_1 \equiv \rho_1/D$ and $K_2 \equiv \rho_2/D$, and they are the inverse of the length scale that characterizes the strength of the surface relaxation. The two peaks indicated by the two arrows are the diagonal signals, due to the two terms $\langle\phi_{1,0}|\phi_{2,0}\rangle$ and $\langle\phi_{1,1}|\phi_{2,1}\rangle$, respectively. Other peaks are off-diagonal signals and the corresponding eigenmodes (p, q) are indicated in the brackets.

When both LK_1 and LK_2 are small, $1/T_{1(2),0} \approx \rho_{1(2)}/L$, $1/T_{1(2),p>0} \approx D(p\pi/L)^2$, the two sets of eigenmodes (T_2 and T_1) are essentially identical and the cross terms become very small. When both LK_1 and LK_2 grow very large, $1/T_{1(2),p} \approx D[(p + 1/2)\pi/L]^2$, the two sets of eigenmodes (T_2 and T_1) become progressively more independent of $\rho_{1(2)}$ and the cross terms again become small. When LK_1 and LK_2 are near unity, the eigenfunctions become sensitive to $K_{1(2)}$, and the cross peak gains weight (if $K_1 \neq K_2$), as shown in Fig. 2.

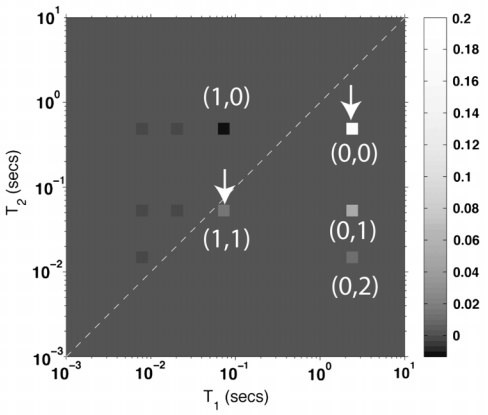

FIG. 1. T_1-T_2 spectrum for a one-dimensional pore of length L with $L\rho_1/D = 0.5$, $L\rho_2/D = 5$, and $L^2/D = 1$ s. The relevant eigenmodes are indicated for some of the peaks. The dashed line is a guide. Note that the cross peaks above the diagonal ($T_2 > T_1$) show a negative sign owing to the structure of the eigenfunctions.

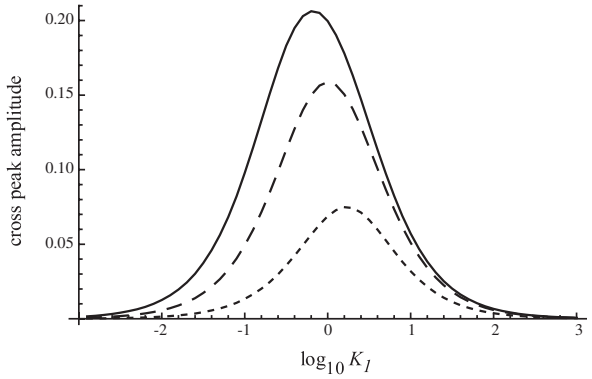

FIG. 2. The overlap integral $\langle\phi_{1,0}|\phi_{2,1}\rangle$ for a range of K_1 and $K_2 = 10K_1$ (solid line), $K_2 = 5K_1$ (dashed line), and $K_2 = 2K_1$ (short-dashed line).

Another type of experiments uses a T_1 relaxation period Δ sandwiched between two T_2 relaxation periods of duration $\tau_2^a = nt_e$ and $\tau_2^b = mt_e$ each:

$$\underbrace{\frac{\pi}{2} - \left[\frac{t_e}{2} - \pi - \frac{t_e}{2}\right]_n - \frac{\pi}{2}}_{T_2 \text{ relaxation } (T_2^a)} - \Delta - \underbrace{\frac{\pi}{2} - \frac{t_e}{2} - [\pi - t_e]_m}_{T_2 \text{ relaxation } (T_2^b)}. \tag{9}$$

This sequence rotates the magnetization at the end of the first T_2 period to be parallel to a static field $\mathbf{B}_0$ by the $\pi/2$ pulse at the end of the period. The magnetization is then allowed to relax for time Δ, a T_1 process. Finally, spin echoes are detected by the CPMG train in the second T_2 relaxation period. Within the framework described above, it is straightforward to write down the evolution of the echo amplitudes for this experiment:

$$M(\tau_2^b, \Delta, \tau_2^a) = \sum_{p,q,r} \langle f|\phi_{2,p}\rangle e^{-\tau_2^b/T_{2,p}} \langle\phi_{2,p}|\phi_{1,r}\rangle \times e^{-\Delta/T_{1,r}} \langle\phi_{1,r}|\phi_{2,q}\rangle e^{-\tau_2^a/T_{2,q}} \langle\phi_{2,q}|i\rangle. \tag{10}$$

Thus, Laplace inversion will result in a 2D spectrum:

$$S_{22}(T_2^b, \Delta, T_2^a) = \sum_{p,q,r} \langle\phi_{2,p}|\phi_{1,r}\rangle\langle\phi_{1,r}|\phi_{2,q}\rangle \times e^{-\Delta/T_{1,r}} \langle f|\phi_{2,p}\rangle\langle\phi_{2,q}|i\rangle \times \delta(T_2^a - T_{2,p})\delta(T_2^b - T_{2,q}). \tag{11}$$

In contrast to the S_{12}, S_{22} now has a user controlled parameter Δ that can be used to manipulate the weight distribution among the modes. For example, when $\Delta = 0$, $\sum_r |\phi_r\rangle e^{-\Delta/T_{1,r}} \langle\phi_r| \to 1$ and thus

$$S_{22}(T_2^a, 0, T_2^b) = \sum_{p,q} \delta_{p,q} \langle f|\phi_{2,p}\rangle\langle\phi_{2,q}|i\rangle \times \delta(T_2^a - T_{2,p})\delta(T_2^b - T_{2,q}), \tag{12}$$

where only diagonal signals survive. When Δ is long, the slowest T_1 mode ($r = 0$) dominates the evolution and the weight distribution will be affected by the nonorthogonality $\langle\phi_{2,p}|\phi_{1,0}\rangle$ between the T_1 and T_2 modes.

An example of a T_2-T_2 single-pore spectrum is shown in Fig. 3. Notice that all peaks are positive and the off-diagonal peaks show a symmetric pattern as is expected from Eq. (11). Peaks on both sides of the diagonal line corresponding to $(p, 0)$ and $(0, p)$ up to $p = 3$ are visible in the plot. The lower panel of Fig. 3 shows the Δ dependence of the off-diagonal peak $(0, 1)$ showing a rapid increase near $\Delta \sim 0$ and a later decay with the time constant of the lowest mode, $T_{1,0} = 2.34$ s. The initial increase is dominated by the $\phi_{1,1}$ mode with a time constant of $T_{1,1} = 0.092$ s. This example with a single pore clearly shows where the main features of the 2D NMR spectrum originate from. The presence of the off-diagonal peaks is due to *nonorthogonality* of T_1 and T_2 modes, which arises from $K_1 \neq K_2$.

Next we examine the spectral effects of interpore connectivity. Recently, T_1-T_2 and T_2-T_2 experiments have been used as a probe for the coupling between different pores [1,2]. Off-diagonal signals were observed in these experiments and interpreted as the signature of the pore-to-pore diffusion exchange. A heuristic time constant τ_{ex} was defined to describe the diffusion between the pores as hopping or chemical exchange.

Here we numerically compute the eigenmodes of Eq. (1) in a coupled two-pore system [15] and show that, in the

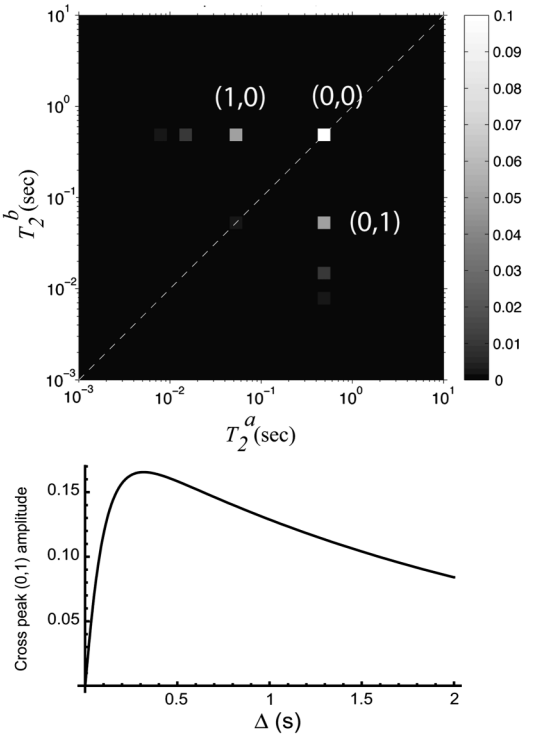

FIG. 3. Top: S_{22} calculated for the 1D-pore model with $LK_1 = 0.5$, $LK_2 = 5$, and $\Delta = 1$ s. Bottom: The amplitude of the off-diagonal peak $(0, 1)$ as a function of Δ.

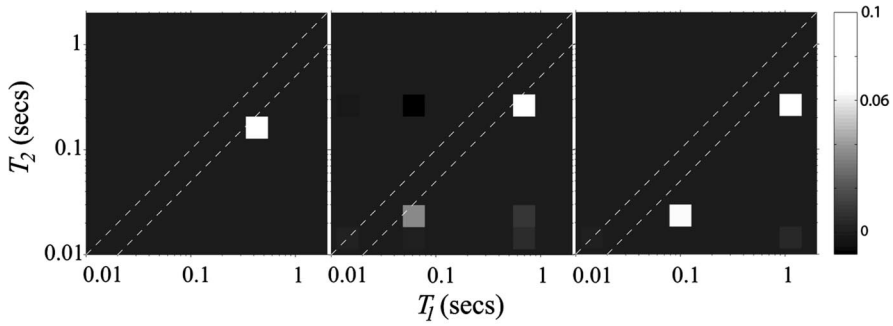

FIG. 4. The 2D NMR T_1-T_2 spectra of coupled pores for different coupling lengths: $L_C/L_A = 10^{-2}$ (left), 5 (middle), and 10^6 (right). $L_A K_1 = 0.5$, $L_A K_2 = 2$, and $L_A^2/D = 1$ s.

T_1-T_2 experiment, the off-diagonal signal can appear in specific diffusion regimes and that it is sensitive to the diffusive coupling. In this model, the diffusion flux between the two pores (A and B) is controlled by an effective coupling length L_C and is given by $\Delta m/L_C$ (Δm is the magnetization difference across the interface). The size ratio of the two pores was chosen to be L_A:L_B = 1:0.121 [15]. In Fig. 4, three regimes of the interpore coupling are shown: $L_C/L_A = 10^{-2}$, 5, and 10^6. At $L_C/L_A = 10^{-2}$ (left panel), the two pores are fully coupled and the diffusion dynamics are similar to a single pore of size $L_A + L_B$; thus, the structure of the 2D spectrum is a single peak. For $L_C/L_A = 10^6$ (right panel), the two pores are uncoupled and the diffusion dynamics of the two pores are independent. Thus, the 2D spectrum is simply the superposition of the two pores, primarily the two peaks corresponding to the relaxation modes in each pore, respectively. The peak at $T_1 \sim 1$ s is from pore A and the peak at $T_1 \sim 0.1$ s is from L_B. A very weak off-diagonal peak at $T_1 \sim 1$ s and $T_2 \sim 0.01$ s is present due to the diffusion within pore A similar to Fig. 1; however, it may not be easily seen in the figure given the scale.

In the intermediate coupling case for L_C/L_A between 1 and 10, the diffusion dynamics are more complex and the spectrum contains more pronounced off-diagonal peaks. As L_C increases, the single peak (left panel) splits into two near the diagonal, one moves to longer T_1 to that of the large pore, and one moves to shorter T_1 toward the small pore. Also, more interestingly, two cross peaks appear at two places: T_1 of L_A and T_2 of L_B (positive), and T_1 of L_B and T_2 of L_A (negative). The amplitude of these peaks grows to a maximum for $L_C/L_A \sim 1$–10 and then decreases for larger L_C. At $L_C/L_A = 10^6$, the two pores are decoupled and thus cross peaks disappear.

Figure 4 shows that the interpore diffusive coupling can significantly accentuate the off-diagonal peaks that may not be visible in a single pore. However, for the appearance of these ''exchange'' cross peaks, just as for the case of a single pore, it is necessary to have $K_1 \neq K_2$.

In conclusion, we described a theoretical framework for the spin dynamics in a general pore system such as cements, rocks, food systems, and granular materials and applied it to a single-pore and two coupled-pores systems in the context of two-dimensional NMR diffusion-relaxation experiments. This framework may accommodate all the relevant diffusion dynamics, such as surface relaxation, membrane permeability, and diffusion between pores. We demonstrated the richness of the diffusion dynamics that could be further explored for real materials with a direct numerical evaluation of eigenmodes [16] as well as random-walk simulations. Such 2D NMR is also important to polymer and colloid sciences [17,18].

[1] L. Monteilhet, J.-P. Korb, J. Mitchell, and P. J. McDonald, Phys. Rev. E **74**, 061404 (2006); http://link.aps.org/abstract/PRE/v74/e061404.
[2] K. E. Washburn and P. T. Callaghan, Phys. Rev. Lett. **97**, 175502 (2006); http://link.aps.org/abstract/PRL/v97/e175502.
[3] A. E. English, K. P. Whittall, M. L. G. Joy, and R. M. Henkelman, Magn. Reson. Med. **22**, 425 (1991).
[4] J.-H. Lee, C. Labadie, C. S. Springer, Jr., and G. S. Harbison, J. Am. Chem. Soc. **115**, 7761 (1993).
[5] H. C. Torrey, Phys. Rev. **104**, 563 (1956).
[6] R. L. Kleinberg, S. A. Farooqui, and M. A. Horsfield, J. Colloid Interface Sci. **158**, 195 (1993).
[7] K. R. Brownstein and C. E. Tarr, Phys. Rev. A **19**, 2446 (1979).
[8] S. Ryu, Magn. Reson. Imaging **19**, 411 (2001).
[9] M. Kac, Am. Math. Mon. **73**, 1 (1966).
[10] Y.-Q. Song, Phys. Rev. Lett. **85**, 3878 (2000).
[11] S. Sridhar and A. Kudrolli, Phys. Rev. Lett. **72**, 2175 (1994).
[12] H. Y. Carr and E. M. Purcell, Phys. Rev. **94**, 630 (1954).
[13] S. Meiboom and D. Gill, Rev. Sci. Instrum. **29**, 688 (1958).
[14] Y.-Q. Song, L. Venkataramanan, M. D. Hurlimann, M. Flaum, P. Frulla, and C. Straley, J. Magn. Reson. **154**, 261 (2002).
[15] L. J. Zielinski, Y.-Q. Song, S. Ryu, and P. N. Sen, J. Chem. Phys. **117**, 5361 (2002).
[16] A. T. de Hoop and M. D. Prange, J. Phys. A **40**, 12463 (2007); http://stacks.iop.org/1751-8121/40/12463.
[17] Y. Qiao, P. Galvosas, T. Adalsteinsson, M. Schönhoff, and P. T. Callaghan, J. Chem. Phys. **122**, 214912 (2005).
[18] P. L. Hubbard, K. M. McGrath, and P. T. Callaghan, Langmuir **21**, 4340 (2005).